Second International Conference on CFD in the Minerals and Process Industries
CSIRO, Melbourne, Australia
6-8 December 1999

2D MODELING OF THE COMBUSTION AND NO_X FORMATION IN FURNACES PRODUCING FESI

Benjamin RAVARY[1] and Stein Tore JOHANSEN[1]

[1] SINTEF Materials Technology, Alfred Getz vei 2B, 7034 Trondheim, NORWAY

ABSTRACT

This paper is a preliminary numerical study of the combustion of CO/SiO gas and NO_x formation, in a Ferro Silicon furnace. A simplified 2D geometry was examined with two positions for the air intake (upper and bottom). Two compositions of the process gas have been considered: only CO and a mixture of CO and SiO. Inputs to this model are either physical data or, parameters that are deduced from former measurements and observations in a Ferro Silicon plant. The calculated distributions of velocity, temperature and species seem physically correct. In the case of the upper intake of air, the jet of air results in a peculiar flow field with gas sucked towards the air inlet. This peculiarity causes SiO_2 to appear also in this region. NO_x formation depends mainly on the temperature distribution in the furnace, which in turn depends on its geometry and in particular the design of air intakes. When SiO is introduced, NO_x formation is increased. This is due to the higher heat of reaction for SiO combustion. The comparison with measurements of NO_x concentration and off gas temperature showed a fair agreement.

NOMENCLATURE

g acceleration of gravity ($m.s^{-2}$),
h characteristic height (m),
q mass flow rate (kg/s)
T temperature (K),
Φ heat flux ($W.m^{-2}$),
ρ density ($kg.m^{-3}$),
$\Delta\rho$ typical difference of density in the domain (kg/m^3).

INTRODUCTION

The Norwegian Ferroalloy Producers Research Association (FFF) has been promoting work in order to understand and to improve the Silicon and Ferro Silicon processes. This research work aims at promoting better furnace operation, energy recovery and lower pollutant emissions in order to meet new stricter environmental regulations.

Comprehensive measurements focusing on the off-gas have been performed on plants (Johansen et al., 1991 and 1998). Johansen et al. (1991) analyzed the mechanisms controlling clogging of off-gas channels from FeSi furnaces and showed that the gas composition and the temperature vary strongly with time. The role of probable avalanches of the charge material along the electrodes and a clear relationship between NO_x concentration and silica dust production were pointed out in a later study (Johansen et al., 1998).

Complementary work to increase the understanding of the process includes numerical modeling of the combustion and NO_x formation. This work is just in its preliminary phase and only very simplified 2D designs were modeled using a CFD code. Although very rough assumptions had to be made, this study led to interesting observations. This basic model opens up the way for more advanced studies. It provides information on an environment otherwise difficult to characterize. Actually, measurements are difficult to perform for practical reasons related to industrial operations and quite extreme and fluctuating conditions in the combustion chamber.

MODEL DESCRIPTION

The model was built using the commercial CFD code FLUENT/UNS version 4.2. This code includes subroutines to evaluate the formation of NO_x.

Main assumptions

Turbulence model

In different parts of the furnace, the Reynolds numbers have been evaluated. They were of the order of magnitude of 10^5 so that the flow is certainly turbulent everywhere. Two models of turbulence were tested: the standard k-ε and the RNG (ReNormalization Group) k-ε models (Yakhot and Orszag, 1986). The standard k-ε model tended to overestimate the mixing so that the results in one of the designs became unrealistic. We believe this is due to an overestimation of the production of kinetic energy, which makes the effective viscosity, and the diffusivity of the species unrealistically large. On the other hand, the RNG k-ε model, which FLUENT® claims is valid for a wider range of problems and which is known to give more physical results, gave distribution of species in better agreement with what was expected. The RNG k-ε model was chosen for this work.

Buoyancy

The criterion to decide whether buoyancy should be included is based on the Richardson number, ratio of the Grashof number on the square of the Reynolds number. Namely, buoyancy is of importance when:

$$Ri = \frac{Gr}{Re^2} = \frac{upwards\ thrust}{inertia\ \ force} = \frac{\Delta\rho g h}{\rho v^2} > 1 \qquad (1)$$

In the combustion chamber of the furnace, the gradient of density is very important because of the presence of both

cold air and hot CO and SiO. Consequently, in this region, the Richardson number showed to be larger than 1. Buoyancy has therefore been included. Its influence was included in both the equations of turbulence kinetic energy and dissipation.

Combustion

The species considered were O_2, N_2 for the air and CO, SiO, CO_2 and SiO_2 for the gas coming out of the charge. Water vapor was not included in this first approach. The influence of volatile compounds was introduced by adding an equivalent quantity of CO. The combustion of the carbon and silicon monoxides were considered:

$$CO + \frac{1}{2} O_2 \rightarrow CO_2 \quad (2)$$

$$SiO + \frac{1}{2} O_2 \rightarrow SiO_2 \quad (3)$$

The enthalpy of formation at 298 K, ΔH_{298} used to compute the heat of reaction of these chemical reactions are summarized in Table 1.

Species	CO	CO_2	SiO	SiO_2
ΔH_{298}	$-1.10.10^8$	$-3.93.10^8$	$-9.84.10^7$	$-9.11.10^8$

Table 1: Enthalpy of formation (J/kmol) of the species involved in combustions. The values for silicon oxides come from (Smithells, 1983).

The reaction rate is assumed to be controlled by mixing of the turbulent eddies containing fluctuating species concentrations, so that "mixed is burned". This assumption is widely used in modeling turbulent combustion processes. Hence, for this first modeling approach the eddy dissipation model of Magnussen and Hjertager (1976) was selected.

Calculations were performed using oxygen-poor air, which could be obtained by mixing air with off-gas. The mixture still contains only nitrogen and oxygen. It has a O_2 mole fraction of 0.15 instead of 0.21 for normal air.

Radiation

In this first approach, radiation was not included.

NO_x formation

NO_x is postprocessed from the combustion simulation. That is to say, it is computed from a given flow field and combustion solution. Consequently, the most important point for a proper evaluation of the NO_x formation is an accurate combustion solution.
Three distinct chemical kinetic processes are responsible for the formation of NO_x; Thermal NO_x, prompt NO_x and fuel NO_x. In this study, only thermal NO_x that was believed to be the main source of NO_x has been included. The rate of formation is computed using the Zel'dovich mechanism with rate constants coming from the survey done by Hanson and Salimian (1984). Since several intermediate species, in particular, O and N, are not available as a result of the combustion model, semi-empirical methods are used to evaluate their concentrations.

Geometry and boundary conditions

A real furnace was used as reference for the most important dimensions (radius of the furnace, height). The actual geometry (with 3 electrodes) was fitted into a cylinder symmetric geometry with the symmetry line through the center of an equivalent electrode. At the bottom of the computational domain the charge materials are located. The combustible gases coming from the process in the furnace below enter this boundary. The outlet and inlet's sizes were chosen to have the same section area as in the real furnace, in order to maintain the values of the average velocities. The resulting geometry is presented in Figure 1.

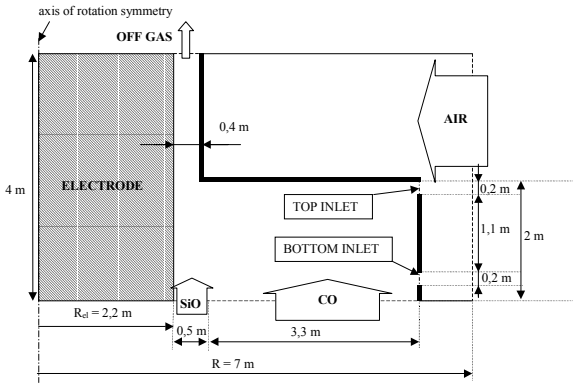

Figure 1: Scheme of the modeled, cylinder symmetrical geometry. Two positions for the inlet of air in the furnace were tested: top inlet or bottom inlet.

When SiO is introduced, its inlet is located close to the electrode, as shown in Figure 1. CO gas is introduced through the main part of the charge material surface, in a ring ranging from radial positions 2.7 m to 6.5 m when SiO is introduced and all along the charge boundary otherwise. The mass flow rates of incoming CO gas and air were deduced from a 35 kg/s outflow rate case based on a real furnace in operation. The temperature of the electrode surface was roughly evaluated from observations on the working furnace. The water-cooled hood walls have a temperature of 500 K. Boundary conditions are summarized in Figure 2.

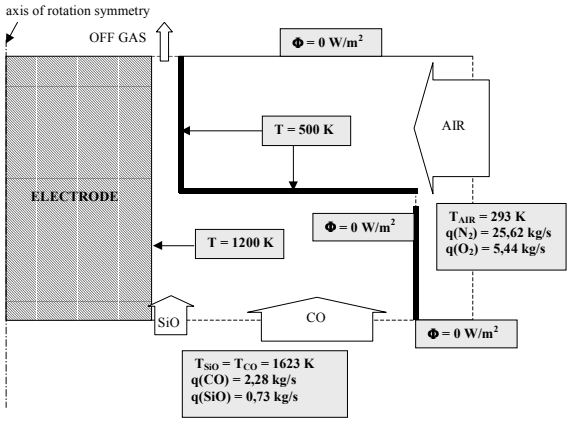

Figure 2: Scheme with the boundary conditions (geometry with the top inlet for air, the boundary conditions remain the same when the inlet is shifted to the bottom). Φ stands for heat flux at the nearby wall.

A 42 x 50 structured mesh was used (42 in z-direction).

RESULTS

The following four simulations have been carried out:

- Only CO gas from the charge and air by the top inlet
- Only CO gas from the charge and air by the bottom inlet
- Both SiO and CO gas from the charge and air by the top inlet
- Both SiO and CO gas from the charge and air by the bottom inlet

All the simulations fully converged. For all parameters, normalized residuals were lower than 10^{-3} and lower than 10^{-6} for temperature and NO_x.

Simulations without SiO

In the off-gas combustion chamber, the jet of air sweeps above the incoming CO. The air mass and volume flow rates are much larger than for CO so that the air forms a zone with high radial inward velocity. The hot products of combustion leave the combustion chamber through the outlet pipe at a high velocity. The maximum velocity is near the electrode where the temperature is high and the density is low.

The acceleration regions are well illustrated by the streamlines (Figure 3). For the top inlet of air, the air jet entrains the furnace gas.

This entrainment rate is balanced by the CO flow supplied from the charge surface If no fluid came from downwards a vortex would develop below the intake, as observed for the bottom inlet. The CO flow prevents the vortex from developing and a peculiar type of streamline is observed coming from the CO inlet.

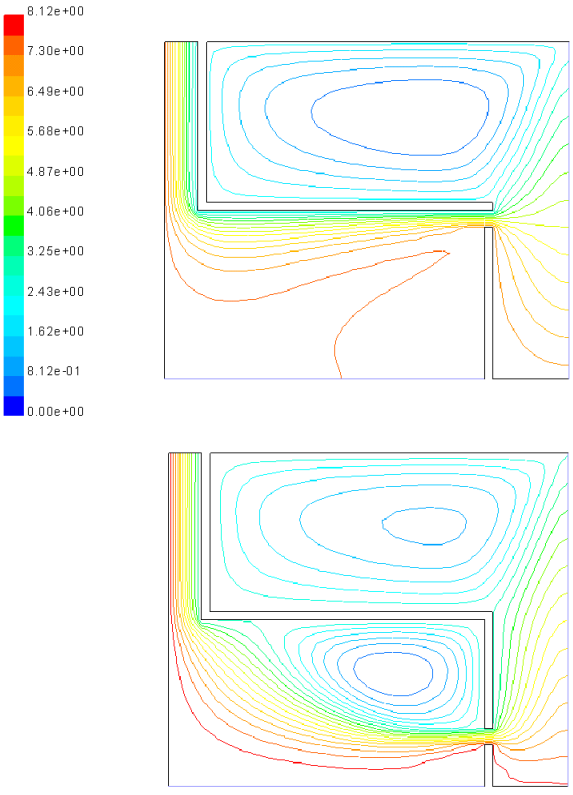

Figure 3: Stream function contours (kg/s) materializing the streamlines without SiO (only CO). Top: top inlet of air; Bottom: bottom inlet of air.

The average temperature at the outlet in both designs is about 1060K, which agrees with the value computed from the overall heat balance, assuming that all CO is burned. The complete combustion of CO is verified when overall species' balance is calculated. As expected, the maximum temperature (around 2700K) is below the adiabatic flame temperature.

In both cases, at the interface between O_2 and CO, in a layer with a thickness depending on the geometry, the combustion generates heat that results in hot zones (Figure 4). The jet of air, which enters in the combustion chamber, has a flow rate much larger than for CO and it is high above the stoichiometric ratio. Consequently, the airflow confines the hot zone below its injection point. As soon as it mixes with CO, CO is burned as a direct result of the selected combustion model. This is why the hot zone occupies a larger region of the combustion chamber when its injection is at the top. This analysis is confirmed by the distribution of species.

The distribution of temperature results in an unstable stratification (cold heavy gas at the top). This distribution can be observed for all the simulations. In unstable stratification, the turbulent energy is augmented by the buoyancy term

In reality, the predicted hot zone close to the air intake for bottom injection is not observed. This is a result of the too low mixing temperature, which prevents combustion due to kinetic limitations.

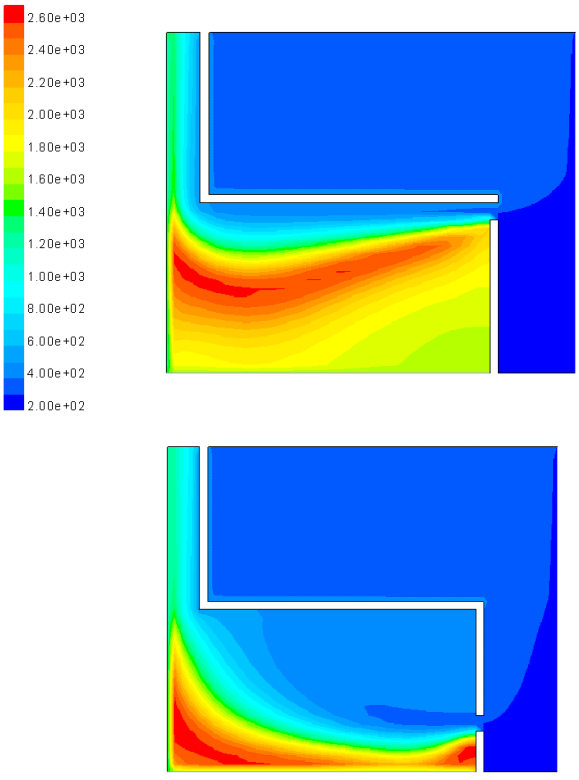

Figure 4: Distribution of temperature (K) without SiO (only CO). Top: top inlet of air. Bottom: bottom inlet of air.

The mixing and the combustion govern the spatial distribution of species. The reason why the hot zone is wider for the top injection of air appears clearly when displaying the distribution of O_2, which is above the CO_2

layers (Figure 5). The cold oxygen in excess results in a cold upper zone, which is wider for the bottom inlet. CO is only present below the CO_2 layers because where the mixing occurs CO is burnt into CO_2. For the bottom inlet, CO disappears very quickly. One of the reasons for this effective combustion is that turbulence, which is enhanced by buoyancy, enhances mixing. In the case of the bottom inlet oxygen is available for carbon materials at the top of the charge and for the lower parts of the electrode. This will result in loss of carbon due to oxidation both from charge and electrode.

The correspondence between the hot zone and the zone of formation of CO_2 is very clear (Figure 5). The flow field in the bottom inlet of air drives some CO towards the center before burning. This characteristic of the flow can explain that a higher mass fraction of CO_2 is reached in this case, near the electrode. In this region, a larger CO flow rate is available and is burned.

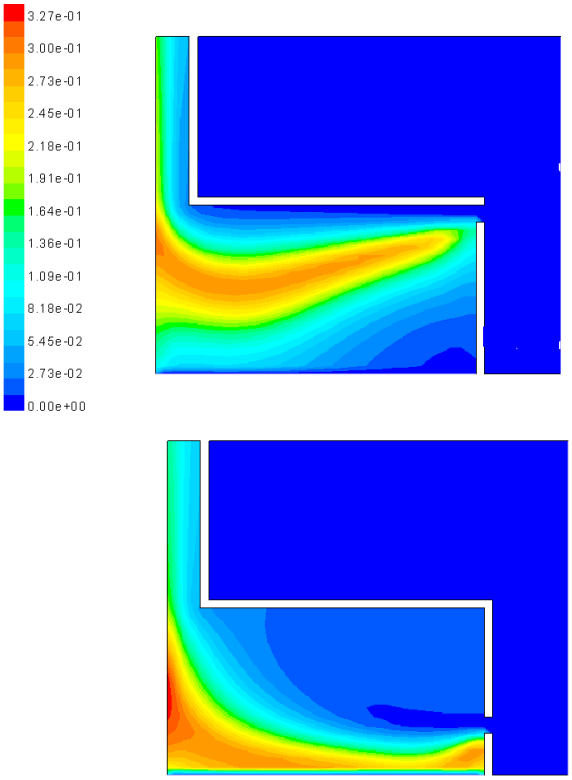

Figure 5: Distribution of mass fraction of CO_2 without SiO (only CO). Top: top inlet of air; Bottom: bottom inlet of air.

Thermal NO_x formation is highly temperature dependent. The total mass flow rates of NO_x at the outlet are similar for both geometries (Table 2). By comparing this result and the distribution of NO_x (Figure 6) with the distribution of temperature (Figure 4), one clearly understands that the key parameter is the spatial and temporal distribution of temperature rather than the average temperature. This fact had been pointed out by the measurements (Johansen et al., 1998) which showed that the NO_x concentration was not directly correlated to the average gas temperature. Indeed, the fact that the hot region is larger for the geometry with the upper inlet does not result in a higher NO_x production. The peak temperatures are reached on larger regions for the bottom inlet so that NO_x production is higher. These differences in temperature distribution are related to the mixing and the combustion: the zone of CO_2 formation (Figure 5) is more homogeneous and larger for the upper inlet of air since the mixing layer has a larger space to develop in this case. On the other hand, for the bottom inlet, the mixing layer is confined between the CO inlet and the airflow and gradients can only be steeper.

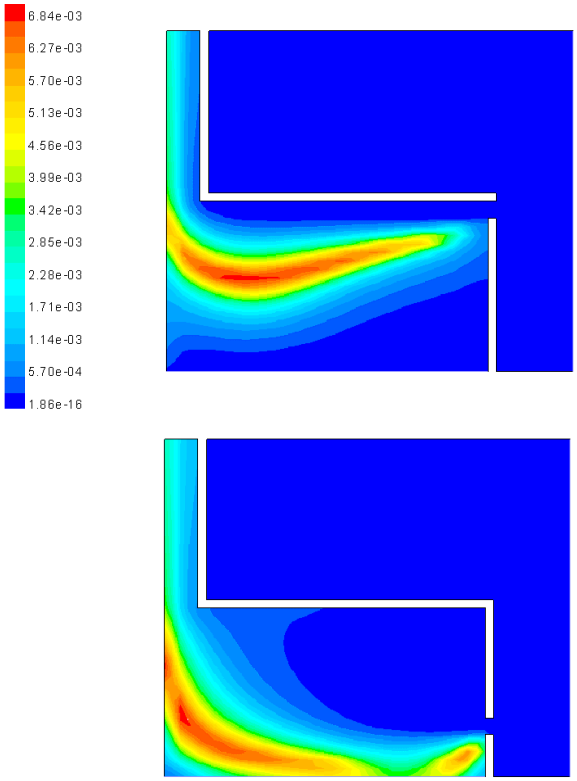

Figure 6: Distribution of mass fraction of NO without SiO (only CO). Top: top inlet of air; Bottom: bottom inlet of air.

Simulations with SiO

The flow has very similar characteristics to the one observed without SiO. Rather low velocities are observed in the combustion chamber and higher velocities correspond to the air jet. The velocity profile in the outlet pipe also shows higher velocities near the electrode. The main difference is the maximum velocity that is higher when SiO is injected. This can be easily explained by the increased mass flow rate (because of the supplementary SiO) and by the higher temperature due to SiO combustion.

The average temperature of the off gas is about 1460 K in both geometries. The difference of temperature between the latter and the former case corresponds to the heat of reaction from the combustion of SiO, which is about twice as large as for CO. It also explains why the maximum temperature is higher. The peak temperature (about 2850 K) is reached above the SiO inlet (0,5 m large ring near the electrode) where the SiO combustion takes place (Figure 7). This maximum temperature is unrealistically large and can be explained by the neglected radiation.

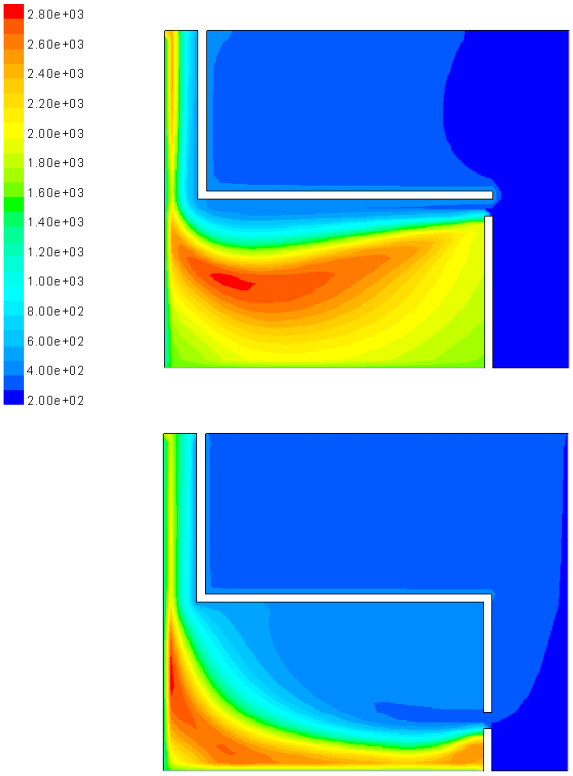

Figure 7: Distribution of temperature (K) with SiO and CO. Top: top inlet of air; Bottom: bottom inlet of air.

For species, the main difference is a lower concentration of O_2 in the outlet pipe that can be explained both by the supplementary combustion due to SiO and dilution. For the top inlet of air, O_2 supply close to the electrode is insufficient. Hence, combustion is not completed in this zone and will continue into the outlet pipe.

All CO is now introduced closer to the inlet of air and the combustion of CO is complete. The distribution of carbon oxides is obviously modified by the presence of silicon oxides near the electrode. Without SiO (Figure 5), the maximum concentration of CO_2 was reached near the electrode (towards which the flow of reactants and products converged). This is no longer the case when SiO is introduced near the electrode. The large CO_2 concentration zones are shifted upwards and radially outwards by the flow of silicon oxides.
Silicon oxides occupy the immediate vicinity of the electrode: SiO at the bottom and SiO_2 at the top. In the case of the bottom inlet of air, the combustion of SiO occurs earlier so that the SiO_2 distribution is more even. The better combustion results in a lower flow rate of SiO at the outlet (0,0014 kg/s instead of 0,015 kg/s for the upper injection of air). For the top inlet of air, the presence of SiO_2 towards the air inlet can be explained by the peculiar streamlines coming from the SiO/CO inlet. Low velocity magnitude in this region and turbulent dispersion also contributes to this spatial distribution.

The production of NO_x is drastically increased by the introduction of SiO (Table 2). The much higher temperatures are due to the higher enthalpy of reaction for SiO. This is in good agreement with experimental observations that NO_x release is highly correlated to silica dust production (Johansen et al., 1998)

	upper air intake	bottom air intake
CO only	0,053 kg/s	0,063 kg/s
	285 ppm	320 ppm
SiO and CO	0,19 kg/s	0,16 kg/s
	900 ppm	640 ppm

Table 2: Net flow rate of NO at the outlet (kg/s) and corresponding concentration in ppm.

The maximum mass fraction of NO_x is now more than 3 times larger than without SiO and this despite dilution phenomena.
The NO_x rich zones are found in the same zones for both pure CO combustion and with SiO combustion. However, the NO_x concentration is larger close to the electrode when SiO is introduced.

Comparison with experiments

Comparison with experiments cannot be really quantitative because of the rough approximations made in the model (in particular concerning the geometry and the boundary conditions) and because of the large temporal fluctuations in the measurements. Moreover, the existing measurements only deal with off gas and consequently no information on distribution is available.
Off gas temperature and concentration of NO_x from Johansen et al. (1998) were compared to the numerical results. The model geometry with the air inlet at the bottom is closest to the real furnace geometry and its numerical results are chosen for comparison.
Measurements from two different days of Ferro Silicon production were in average quite similar. The time dependent NO_x concentration in the off gas varies from 100 ppm to just under than 600 ppm (Figure 8). The lowest value corresponds to low dust and only CO out of the furnace (no SiO). Numerically, in this case, the concentration is 280 ppm so that the production of NO_x is over predicted. With SiO, the model gives a concentration of 680 ppm that is also higher than the average concentration found experimentally. This difference must be due to an over estimation of the temperature in the furnace. Three main explanations can be pointed out:
i) The water vapor that was not included in the model would increase the specific heat and as a result decrease the temperature.
ii) Radiation that was not taken into account would allow a quicker drainage of heat from the flame zones.
iii) The omission of reaction kinetics will overestimate combustion rates in some zones.
iv) Above 2500 K, SiO_2 vapor may exist according to thermodynamic calculations. The vaporization of SiO_2 was not accounted for and would result in a decrease of the temperature.

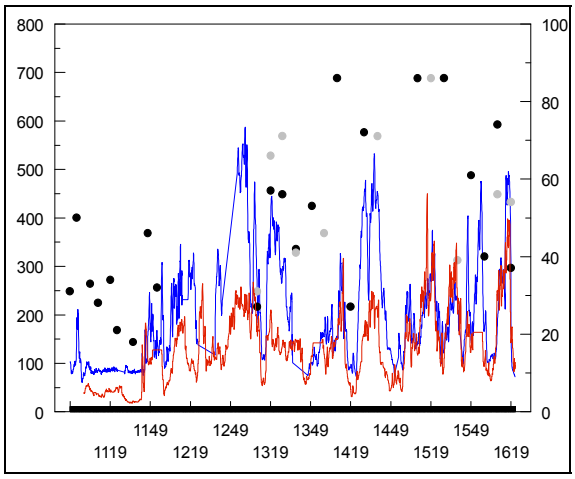

Figure 8: Concentration of NO_x (upper curve) and dust (lower curve) (ppm) as a function of time (h:min)

The off gas temperatures measured are in average about 1000 K (Figure 9), which are lower than the computed temperatures without SiO (1060 K) and with SiO (1450 K). This confirms our previous analysis about the NO_x formation.

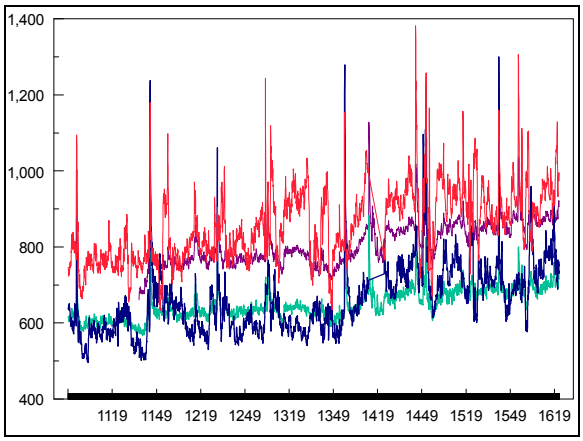

Figure 9: Off gas temperature (^oC) measured at different points in the furnace as a function of time (h:min).

CONCLUSION

This study is a preliminary work to model combustion and NO_x formation in a Ferro Silicon furnace. It is based on an idealized simplified geometry in order to understand the main physical phenomena involved and to evaluate the models included in FLUENT/UNS. The main conclusions of this study are:

1) Position of the inlet of air has an influence on the highly temperature dependent NO_x formation. The distribution rather than the average of temperature is of importance. By performing a good mixing and even combustion, peaks of temperature are reduced, resulting in lower NO_x emissions.
2) The predicted overall distribution of temperature and species seem physically correct but no experimental data is available to confirm this result. Buoyancy was included.
3) The introduction of SiO results in higher local temperatures because of a higher heat of combustion than CO. As a result, the NO_x concentration in ppm is more than twice as high compared to the case without SiO. This result is in accordance with experimental observations.
4) Numerical results are in fair agreement with measurements of temperature and NO_x concentration. The model over estimates both the NO_x formation and the temperature.
5) The bottom inlet of air will result in higher oxidation of carbon for charge materials and electrodes.
6) In order to improve the accuracy of the model the following points should be considered:

- addition of water vapor to the air,
- modeling of the radiative transfers from the soot to the walls,
- 3D simulation to account for the formation of thermal plumes from SiO which normally is observed in real furnaces,
- introduce a better combustion model which accounts for the interaction of kinetics and turbulence (Gammelsæter, 1997).

ACKNOWLEDGEMENTS

The Norwegian Ferroalloy Producers Research Association (which includes Elkem, FESIL and Tinfos) is acknowledged for their financial support.

REFERENCES

GAMMELSAETER, H. R., (1997). "Modeling of structural efffects on chemical reaction in turbulent flows", Dr. Ing. Thesis, NTNU, Trondheim, Norway.

HANSON, R.K. and SALIMIAN, S., (1984) "Survey of rate constants in H/N/O systems", in *Combustion Chemistry*, W.C. Gardner editor, 361.

JOHANSEN, S.T., GRAADAHL, S., GAMMELSAETER, R., RAANES, M., ARNTSBERG, A.E., LINDSTAD, T., ENSTAD, G. AND TVEIT H. "Clogging of Ferro-silicon furnace off-gas channels at high temperatures", (1991) Smelter Process Gas Handling and Treatment, Ed. T.J.A.: Smith and C. J. Newman, The Minerals, Metals & Materials Society, 7-18.

JOHANSEN, S.T., GRAADAHL, S., BYBERG, J.AA., TVEIT, H. and WALDERHAUG, AA., (1998) "Environmental aspects of Ferro-Silicon furnace operations - an investigation of waste gas dynamics", *Proceedings INFACON 8*, Beijing, 7.-10. June.

MAGNUSSEN, B.F. and HJERTAGER, B.H. (1976) "On mathematical models of turbulent combustion with special emphasis on soot formation and combustion", *16th Symp. on Combustion*, Cambridge, MA, USA.

SMITHELLS, C.J., (1983) "Smithells metals reference book", Sixth Edition, Brandes, E.A., (editor), Butterworth.

YAKHOT, V. and ORSZAG, S.A. (1986), "Renormalization Group Analysis of Turbulence: I. Basic Theory", *J. Scientific Computing*, 1(1), 1-51.